

Relative Age Estimation Using Face Images

Ran Sandhaus, Yosi Keller*

Abstract—This work introduces a novel deep-learning approach for estimating age from a single facial image by refining an initial age estimate. The refinement leverages a reference face database of individuals with similar ages and appearances. We employ a network that estimates age differences between an input image and reference images with known ages, thus refining the initial estimate. Our method explicitly models age-dependent facial variations using differential regression, yielding improved accuracy compared to conventional absolute age estimation. Additionally, we introduce an age augmentation scheme that iteratively refines initial age estimates by modeling their error distribution during training. This iterative approach further enhances the initial estimates. Our approach surpasses existing methods, achieving state-of-the-art accuracy on the MORPH II and CACD datasets. Furthermore, we examine the biases inherent in contemporary state-of-the-art age estimation techniques.

I. INTRODUCTION

Facial images are a primary modality for age estimation in human perception and automated systems. In computer vision and biometrics, significant research has focused on age estimation from facial images, with applications in e-commerce [1], facial recognition [2], and age-based data retrieval. However, accurately estimating age from facial images remains challenging due to the complex and heterogeneous facial transformations occurring due to aging. Ethnicity, gender, and lifestyle are significant factors influencing these changes. Aging results in progressive facial features and appearance transformations, where individuals of similar ages often appear comparable, while those of larger age differences result in more pronounced distinctions [3].

To address these challenges, face-based age estimation is typically formulated as a classification task, assigning a facial query image \mathbf{x}_q to discrete age categories $\{a_c\}_1^C$ [4], [5], [6], [7], [8], [9], or as a regression task, treating age as a continuous variable $a \in \mathbb{R}^+$ [5], [9], [4], [10], [11], [12]. Face-based biometric analysis starts by aligning a facial image to a canonical spatial frame [8], followed by analyzing the cropped region of interest. Early methods utilized local image descriptors [8] to encode facial images into high-dimensional representations for age regression via kernel PLS [5].

In the past decade, advancements in deep learning have enabled the development of end-to-end trainable age estimation schemes [13], [14] that utilize classification and regression losses. Metric learning approaches have been employed in both shallow [15] and CNN-based schemes [13], [16], [17], where local features of facial images were learned by treating age difference as a metric measure. In contrast, ranking-based approaches [18], [19], [20], [21] leveraged ordinal

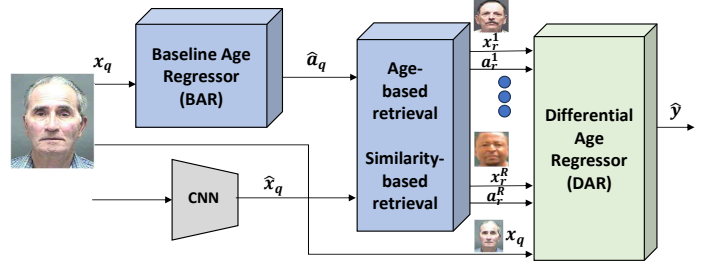


Fig. 1: **Differential age estimation.** The Baseline Age Regressor (BAR) estimates the age \hat{a}_q of the input image \mathbf{x}_q . $\hat{\mathbf{x}}_q$ is the CNN embedding of \mathbf{x}_q used with \hat{a}_q to retrieve the set of reference images that are of age \hat{a}_q and most visually similar to \mathbf{x}_q . The ages of the reference images are known. The Differential Age Regressor (DAR) estimates the age differences between \mathbf{x}_q and the reference images and uses them to refine \hat{a}_q .

classification to exploit the ordinal structure of age labels for improved accuracy. Recent methods have integrated classification and regression techniques [22], as well as attention-based approaches [22], [23], [24], [25]. Despite these advancements, age estimation has predominantly been approached as predicting a person’s age solely from their facial image. While estimating age differences between facial images has the potential to improve accuracy by leveraging the continuous nature of aging, this approach has not yet been integrated into an absolute age estimation framework.

In this work, we propose a novel approach to age estimation, illustrated in Fig. 1. Our method enhances a Baseline Age Regression (BAR) by training a Differential Age Regression (DAR) model using nearest-neighbor (NN) reference facial images from the training set. Estimating age differences using images within small age ranges improves accuracy by addressing the age-varying characteristics of face-based age estimation. State-of-the-art (SOTA) BARs typically achieve an accuracy of $\Delta_{BAR} \sim [15, 70]$, while our DAR model focuses on estimating residual errors within the narrower range of $\Delta_{DAR} \sim [-3, +3]$, thereby refining the BAR estimate. Given the complexity and variability of visual aging patterns in facial images, and considering that $\Delta_{BAR} \gg \Delta_{DAR}$, our DAR model demonstrates superior accuracy compared to traditional BAR methods. To our knowledge, this is the first differential-based age estimation method that evaluates age differences between a query image and a set of reference images. For a given query face image \mathbf{x}_q , we retrieve reference images $\{\mathbf{x}_r\}_1^R$ from the training set based on the BAR estimate of \mathbf{x}_q and facial similarity metrics. The DAR model then estimates the age differences $\{d_r\}_1^R$. The ages of the reference images

R. Sandhaus and Y. Keller are with the Faculty of Engineering, Bar Ilan University, Ramat-Gan, Israel. Email: yosi.keller@gmail.com

are known during both training and testing phases, and the refined age estimate is obtained as a weighted sum of the estimated age differences. We also propose an age-augmentation approach, in which, instead of using the BAR directly, we estimate its error distribution around a_q , denoted as D_ε , and sample $a_q + \varepsilon$, $\varepsilon \sim D_\varepsilon$ to derive an initial age estimate for retrieving the reference set. Furthermore, we demonstrate that iteratively estimating D_ε improves the accuracy of the DAR model. The proposed differential age estimation framework is model-agnostic and can be integrated with any general regression model to enhance prediction accuracy.

To conclude, we summarize our contributions as follows:

- We introduce a novel differential-based age estimation method by estimating age differences between facial images.
- By estimating the age differences between an input image and a set of reference images, we derive a robust and accurate age estimate.
- We propose an age-augmentation approach that models the error distribution of the underlying BAR age estimator and samples it to enhance accuracy.
- The differential age estimation process is iteratively improved by refining the error distribution over training epochs.
- The proposed scheme achieves state-of-the-art (SOTA) accuracy on the MORPH II [26] and CACD [27] age estimation datasets.

II. RELATED WORK

Facial age estimation is inherently complex due to significant variations in aging characteristics across ethnicities, genders, and lifestyles [28]. Buolamwini and Gebru [29] demonstrated the significance of ethnicity and gender in face analysis and recognition. Guo and Mu [9] introduced a hierarchical approach wherein facial images are first classified by gender and ethnicity, followed by age estimation within each subgroup to enhance prediction accuracy. Earlier approaches relied on local image features to embed facial images, followed by statistical inference. Balmaseda et al. [8] used Local Binary Pattern (LBP) features and SVM classifiers to analyze multiscale normalized face images and their local context. Zheng and Sun [7] employed a ranking SVM to estimate age by learning ranking relationships, which were then applied to a reference set for age estimation. A gender and age classification scheme was introduced by Eidinger et al. [4] for non-frontal facial images captured under uncontrolled conditions. Regression-based approaches reformulate age estimation as a scalar regression problem using high-dimensional image embeddings. Thus, a regression model for unbalanced and sparse data was proposed by Chen and Gong [11], enabling accurate age and crowd density estimation. Low-level visual features extracted from unbalanced and sparse images were mapped onto a cumulative attribute space, where each dimension corresponds to a semantic interpretation.

While early methods relied on handcrafted features and statistical models, the advent of deep learning has significantly transformed facial age estimation, enabling more robust and

data-driven approaches. A hierarchical unsupervised neural network model was introduced by Wang and Kamikaze [10] to extract robust facial representations. These features were subsequently processed by Recursive Neural Networks (RNNs) to capture age progression patterns. Manifold learning was applied to capture the underlying facial aging manifold by projecting the feature vector into a lower-dimensional, more discriminative subspace. Hasner and Levi [12] improved the accuracy of age estimation by formulating it as a classification problem and leveraging Convolutional Neural Networks (CNNs), while Sendik and Keller [14] applied deep metric learning to CNN-computed facial features and employed a Support Vector Regressor (SVR) for age estimation. Deep metric-learning was also used by Lieu et al. [18] who introduced a hard quadruplet mining scheme to enhance embeddings, applying a regression-based loss for age estimation. Rote et al. [30] developed a classification scheme in which the class probability distribution from the Softmax function was used to compute the empirical expectancy of the estimated age. Pan et al. [31] proposed a multitask approach, where the empirical probability of each age was computed using the Softmax activation function. They minimized both the L_2 loss and the empirical variance of the age estimation error. A set of CNN-based classification models was suggested by Malli et al. [32]. Each model was trained to classify within a specific age range. The final age estimate was obtained by averaging the outputs of these models.

Shen et al. [33] proposed a hybrid Deep Regression Forests approach that combines Regression Forests and deep learning inference. In this method, the forest nodes, which learn adaptive data partitions from the input, are connected to fully connected layers of a Convolutional Neural Network (CNN). The Random Forests and CNN are optimized jointly in an end-to-end manner. A tree-based structure was introduced by Li et al. [34] where adjacent tree leaves in close branches were connected to create a continuous transition. Additionally, they employed an ensemble of local regressors, with each leaf linked to a specific local regressor. The age labels in this approach were encoded using an ordinal-preserving representation [18], [19], [20], [35] to exploit the inherent order of age labels. This encoding ensures that each model outputs signals indicating whether an estimated age exceeds a given threshold. These methods have been shown to improve the accuracy of age classification.

Niu et al. [19] employed an ordinal regression Convolutional Neural Network (CNN) to address non-stationarity in aging patterns and develop the Asian Face Age Dataset (AFAD), which contains more than 160,000 images with accurately labeled ages. The Deep Cross-Population (DC) domain adaptation approach by Li et al. [16] for age estimation trains a CNN on a large source dataset to enhance the accuracy of age estimation on a smaller target dataset. In the DC approach, transferable aging features are learned from the source dataset and then transferred to the target dataset. Additionally, an order-preserving pairwise loss function is utilized to align the aging features of the two populations. Tain et al. [17] proposed a correlation learning method to represent and utilize inter- and intra-cumulative attribute relationships, which was

further extended to perform gender-aware age estimations by leveraging correlations both between and within gender groups.

Attention-based learning has revolutionized NLP-related tasks and was also adapted for computer vision. Hiba and Keller [22] introduced a Deep Learning framework for age estimation, featuring an attention-based image augmentation-aggregation approach and a hierarchical probabilistic regression model. While this approach used attention on top of the augmentations, Wang et al. [23] used attention to identify image patches that should be focused on for age estimation, creating a framework of two CNNs: Attention and Fusionist. Attention employs a novel OMAHA (Ranking-guided Multi-Head Hybrid Attention) mechanism to dynamically locate and rank age-specific patches, which Fusionist integrates with facial images to predict subject age. Line et al. [24] presented an age estimation method for in-the-wild scenarios, incorporating facial semantics through a face parsing-based network and attention module. Considering related tasks in video processing, Deformer, a video-based model for age classification was proposed by Ali et al. [25], that categorizes individuals into four age groups. Addressing challenges like occlusions and low resolution, the method employs a two-stream architecture with the Transformer and EfficientNet architectures.

Sun et al. [36] addressed age estimation challenges such as illumination, pose, expression, and the ambiguity of the age labels between demographic groups. They proposed a general label distribution learning (DLL) formulation that unifies various age estimation methods. Introducing a deep conditional distribution learning (DL) method within this framework, the authors utilized auxiliary face attributes to learn age-related features. From another perspective, considering the inherent imbalance prevalent across datasets, Boa et al. [37] proposed a unified framework for facial age estimation, addressing challenges in both general and long-tailed age estimation. They introduced feature rearrangement, pixel-level adjunct learning, and adaptive routing to enhance performance across diverse age classes. Siamese graph learning (SGD) was introduced by Lieu et al. [38] to address aging dataset bias. SGD aligns sparse and dense distributions, preserving the smoothness of aging. The approach employs a blending strategy for plausible hallucinatory sample generation using unlabeled data and introduces graph contrastive regularization to mitigate noise from auxiliary samples. Generative AI as in Delta Age AGAIN (DAA), was proposed by Chen et al. [39] for age recognition using transfer learning. The DAA operation based on mean and standard deviation values of style maps employs binary code mapping and a FaceEncoder-AgeDecoder framework.

Several image datasets have been used in face-based age estimation. Some older datasets, such as FERET [40] (14K images), FG-NET [41] (1K images), Chalearn LAP 2015 [42] (7.5K images), and UTKFace [43] (16K images), are too small for CNN-based approaches, while others, like IMDB-Wiki [30], are based on web scraping and human age annotators without objective groundtruth age labels. As the accuracy of computational age estimation improves ($MAE \approx 2.5$ years), it becomes comparable to human annotations, limiting their

effectiveness for future work. The MORPH Album II [44] is notable as it provides accurate age and identity labels, while other datasets, including AFAD [19], do not provide identity labels. This has led some works to use only the Random-Split (RS) test protocol, where the image set is randomly split into train and test subsets. As most datasets have 25 images of each subject, this inevitably results in significant train-to-test leakage, making their age estimation results less reliable. In this work, we focus on datasets equipped with identity labels, and use the Subject-Exclusive (SE) protocol, where all of a particular subject’s face images are used just in either the train or test sets.

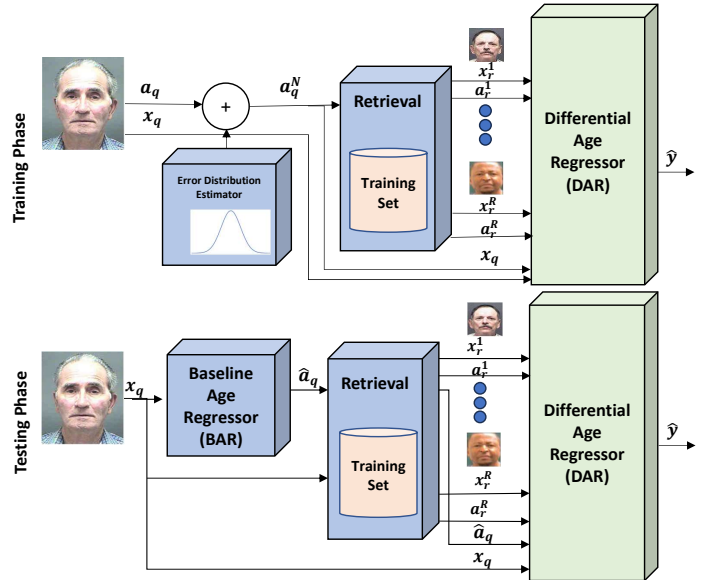


Fig. 2: **Differential age estimation in the training and test phases.** In training time, the groundtruth age a_q of the input face image x_q , is augmented using Eq. 1 and used to retrieve the reference set of images $\{x_r\}_1^R$. In the test phase, a Baseline Age Regressor (BAR) estimates \hat{a}_q , the age of x_q that is used to retrieve $\{x_r\}_1^R$.

III. DIFFERENTIAL AGE ESTIMATION

We propose a novel framework for facial age estimation, leveraging differential age estimation to refine initial predictions. This approach, illustrated in Fig. 2, reduces prediction errors by modeling relative age differences rather than absolute estimates. Given a query image x_q , we first obtain an initial age estimate \hat{a}_q using a Baseline Age Regressor (BAR). To refine \hat{a}_q , we retrieve a reference set $\{x_r\}_1^R$ of individuals with known ages similar to x_q . The Differential Age Regressor (DAR) then estimates the age differences $\{\Delta_r\}_1^R$ between x_q and $\{x_r\}_1^R$, which are used to adjust the final prediction. The reference images are retrieved based on two criteria detailed in Section III-A: (1) its known age a_r is within a bounded range of \hat{a}_q , and (2) it exhibits high visual similarity to x_q in feature space.

Since initial age estimates are subject to systematic errors, we model the error distribution D_ε for robust reference

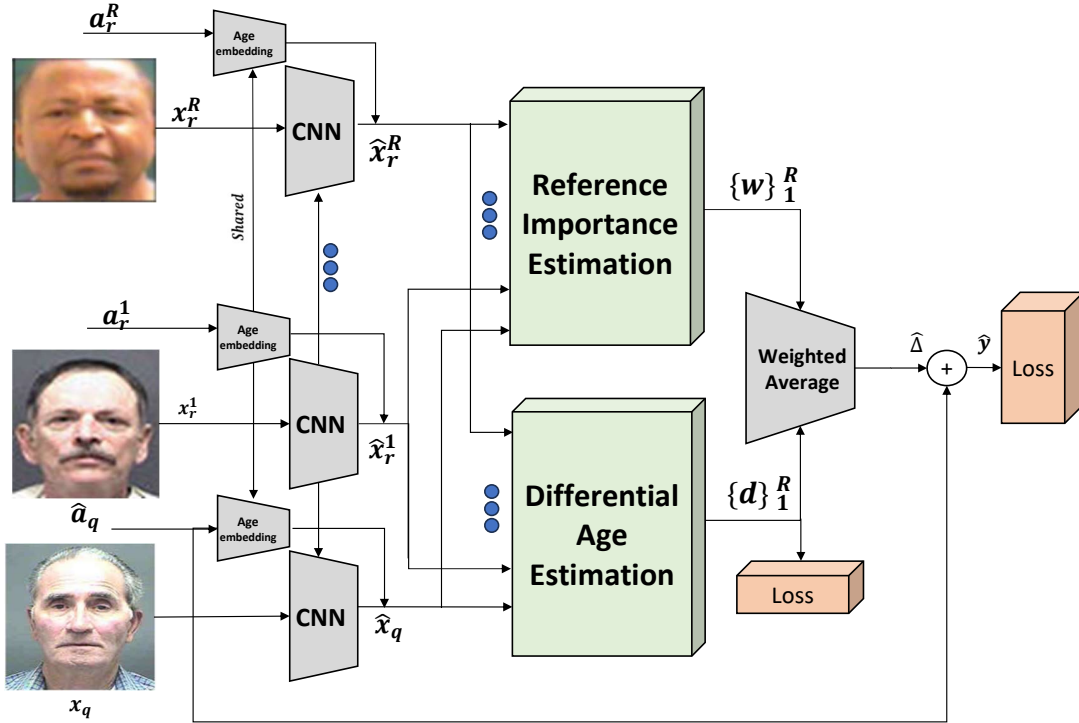


Fig. 3: **The Differential Age Regressor (DAR) network.** The embeddings of the query image x_q and the reference images $\{x_r\}_1^R$ are computed by a CNN, while the initial age estimate of the query image \hat{a}_q and reference ages $\{a_r\}_1^R$ are encoded by an embedding layer. The embeddings are concatenated to \hat{x}_q and $\{\hat{x}_r\}_1^R$. The DAR network uses the embeddings to estimate the age differences $\{d_r\}_1^R$ and the weights per reference $\{w_r\}_1^R$. The resulting difference estimate $\hat{\Delta}$ is the weighted average $\hat{\Delta} = \sum_r w_r d_r$, added to \hat{a}_q to compute the age estimate.

selection, and sample from $a_q + \varepsilon$, $\varepsilon \sim D_\varepsilon$. The DAR estimates the age differences $\{\Delta_r\}_1^R = \{a_q - a_{x_r}\}_1^R$, and the refined age estimate \hat{y} (Eq. 2) as a weighted sum of $\{\Delta_r\}_1^R$. We use the BAR by Hiba and Keller [22] due to its SOTA accuracy. However, our framework is adaptable and can be integrated with any BAR to refine its predictions. The DAR model is implemented using the Convolutional Neural Network (CNN) architecture shown in Fig. 3 and detailed in Section III-B. Additionally, in Section III-D, we demonstrate how to iteratively improve the DAR estimate by refining D_ε and adjusting the sampling of reference training images.

A. Reference Images Retrieval

For each query image x_q , we retrieve an initial candidate set of reference images $\{x_r\}_1^K$ from the training set using the BAR’s estimated age \hat{a}_q , as shown in Fig. 4. We then refine this set by selecting the top $P \ll K$ images most visually similar to x_q using a face embedding network. Directly using \hat{a}_q for reference retrieval may introduce systematic bias due to inherent BAR errors. To mitigate this, we estimate an error distribution D_ε around the true age a_q , enabling more robust reference selection:

$$\hat{a}_q = a_q + \varepsilon, \quad \varepsilon \sim D_\varepsilon \quad (1)$$

and retrieve all reference images $\{x_r\}_1^K$ whose age is \hat{a}_q . By incorporating D_ε , we effectively account for the BAR’s

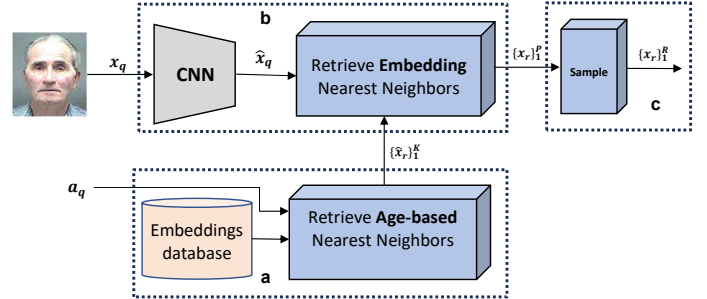


Fig. 4: **Reference faces retrieval.** (a) The age a_q of x_q is used to retrieve $\{\hat{x}_r\}_1^K$ the embeddings of the reference images of the same age. (b) \hat{x}_q , the embedding of x_q is used to retrieve $\{\hat{x}_r\}_1^P$, $P \ll K$, the P embeddings in $\{\hat{x}_r\}_1^K$ closest to \hat{x}_q . (c) We randomly sample $R < P$ images for the final reference set $\{x_r\}_1^R$.

prediction uncertainty, leading to a reference set that is more representative of possible true ages. Since individuals of the same age can exhibit significant facial variations due to gender, ethnicity, and lifestyle factors, we employ a deep face embedding network to refine the reference selection. This ensures that the final reference set is age-consistent and visually coherent. Therefore, given the initial age-retrieved reference

set $\{\mathbf{x}_r\}_1^K$, where $K \gg R$, we utilize a face embedding network [45] to retrieve $\{\mathbf{x}_r\}_1^P$, where $P \gg R$, consisting of the faces most visually similar to \mathbf{x}_q . To prevent overfitting and ensure diverse references, we randomly sample R faces from the visually closest subset $\{\mathbf{x}_r\}_1^P$. This balances precision with robustness, improves the diversity of the training set, and mitigates overfitting. Additionally, we experimented with alternative sampling methods in Section IV-B.

The face recognition model is based on the convolutional portion of VGG16, with the first fully connected (FC) layer removed and a 1D batch normalization layer added to mitigate overfitting. During testing, the same retrieval process is repeated without using Eq. 1, ensuring that $\hat{a}_q = a_q$. The BAR's out-of-sample error distribution D_ε is estimated using Kernel Density Estimation (KDE) [46], applied to a subset of 2% of the dataset sampled in a randomized, subject-exclusive (SE) manner. In practice, we restricted $D_\varepsilon \in [-20, +20]$, as due to the limited number of data points where $D_\varepsilon \notin [-20, +20]$ the KDE-based estimation was inconsistent.

B. Differential Age Regression Network

The Differential Age Regression (DAR) network estimates age differences between a query image \mathbf{x}_q and a set of reference images $\{\mathbf{x}_r\}_1^R$. The model is jointly trained to predict the age differences and the resulting absolute age. The DAR architecture (Fig. 3) processes input images $\{\mathbf{x}_q, \{\mathbf{x}_r\}_1^R\}$ through a convolutional neural network (CNN) backbone. The CNN extracts embeddings, which are concatenated with age embeddings derived from the reference images' known ages. This joint representation $\{\hat{\mathbf{x}}_q, \hat{\mathbf{x}}_r\}_1^R$ is passed to the Differential Age Estimation (DAE) network for age difference prediction. $\{\hat{\mathbf{x}}_q, \hat{\mathbf{x}}_r\}_1^R$ are passed *in parallel* to the Differential Age Estimation (DAE) network, shown in Fig. 5. The DAE estimates the age difference d_r and corresponding weight w_r , respectively, for *each pair separately*. The final age estimate \hat{y} is computed as a weighted sum of predicted age differences d_r . The weights w_r are learned through the DAE network, prioritizing references with higher visual similarity and smaller prediction variance:

$$\hat{y} = \hat{a}_q + \sum_1^R w_r d_r, \quad (2)$$

where \hat{a}_q is the BAR's initial age estimate.

In addition to *first-order* age difference estimation d_r , the model further refines predictions by computing *second-order differentials* d_c , capturing local aging trends. The input images $\hat{\mathbf{x}}_q, \hat{\mathbf{x}}_r$ to the DAE network (Fig. 5) are initially passed through a 3-layer MLP (FC + LeakyReLU + Dropout) with FC layers of dimensions 2048, 1024, and 512, and a Dropout with $p = 20\%$. It employs a weighted regression scheme where a set of regression heads $\{R_c\}_{-C}^C$, with $C = 20$, estimate the second order age differentials $\{d_c\}_{-C}^C$ around the difference values $\mathbb{C} = \{-C, -C + 1, \dots, C - 1, C\}$. $\{d_c\}_{-C}^C$ are merged by computing the weights $\{w_c\}_{-C}^C$ using FC_w and a Softmax such that

$$w_c = P(\text{differential}\{\hat{\mathbf{x}}_q, \hat{\mathbf{x}}_r\} = c). \quad (3)$$

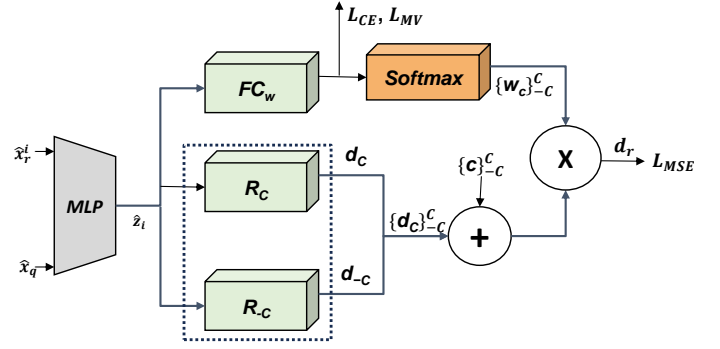


Fig. 5: **Differential Age Estimation.** This network estimates the age differential between the query image $\hat{\mathbf{x}}_q$ and a *single* reference image $\hat{\mathbf{x}}$. Their embeddings are concatenated as pairs $\{\hat{\mathbf{x}}_q, \hat{\mathbf{x}}_r^i\}$. A set of regressors $\{R_c\}_{-C}^C$ estimates $\{d_c\}_{-C}^C$: the *second-order* age differentials *around* $\{c\}_{-C}^C$. $\{d_c\}_{-C}^C$ are weighed by $\{w_c\}_{-C}^C$ computed by FC_w and a Softmax layer as in Eq. 4.

Thus, the age differential d_r between $\hat{\mathbf{x}}_q$ and $\hat{\mathbf{x}}_r$ is given by the weighted average:

$$d_r = \sum_{-C}^C w_c \cdot (c + d_c). \quad (4)$$

Equation 4 is estimated for all R image pairs $\{\hat{\mathbf{x}}_q, \hat{\mathbf{x}}_r\}_1^R$ to compute the *first-order* differentials $\{d_r\}_1^R$, that are merged in a weighted average using the weights $\{w_r\}_1^R$ to compute the absolute age estimate \hat{y} as in Eq. 2.

C. Model Training

Unlike standard absolute regressors, our model simultaneously optimizes absolute age predictions and relative age differences. This multitask approach improves generalization by leveraging local and global aging patterns, leading to more stable and accurate predictions. Thus, the DAR model is trained using multiple losses. Both the query age estimation \hat{y} and the age differences $\{d_r\}_1^R$ are jointly optimized, while the absolute age estimation \hat{y} is optimized with an MSE loss, denoted L_{MSE}^a . Each age difference estimate, d_r , is optimized using multiple loss terms. The Cross-Entropy Loss $L_{CE}^{d_i}$ ensures classification probabilities in Eq. 3, while the Mean-Variance Loss components $L_M^{d_i}$ and $L_V^{d_i}$ minimize prediction variance [31]. The regression results of the reference age difference are optimized with an MSE loss $L_{MSE}^{d_i}$. Since age differences between two images should be symmetric, we enforce the constraint $\Delta(\mathbf{x}_1, \mathbf{x}_2) = -\Delta(\mathbf{x}_2, \mathbf{x}_1)$. This constraint is incorporated during training by applying the DAR network to both query-reference pairs in opposite directions, enhancing prediction consistency. After defining individual loss terms, we combine them into a unified objective function that balances absolute and differential predictions

$$L = L_{MSE}^a + \frac{1}{R} \sum_{i=1}^R (L_{CE}^{d_i} + L_M^{d_i} + L_V^{d_i} + L_{MSE}^{d_i} + L_{MSE}^a). \quad (5)$$

The $L_{MSE}^{d_i}$ regression losses of the age difference relate to both asymmetric age regressions.

D. Iterative DAR Refinement

Since the Baseline Age Regressor (BAR) is prone to systematic estimation errors, we iteratively refine its predictions using the Differential Age Regressor (DAR). By modeling the BAR’s error distribution D_ϵ and updating it with each iteration, the age estimation process progressively improves in accuracy. We employ an iterative refinement strategy where the updated BAR predictions at each step serve as input for the next iteration, effectively cascading the improvements over multiple refinements D_ϵ^n , progressively reducing prediction errors

$$BAR_{n+1}(D_\epsilon^{n+1}) = DAR(BAR_n, D_\epsilon^n), \quad (6)$$

where BAR_0 is the initial absolute age estimator and D_ϵ^0 as its associated error estimate. At each iteration n , the error distribution D_ϵ^n is updated, refining the BAR predictions iteratively. This has been experimentally shown in Section IV-B to improve age estimation accuracy.

IV. EXPERIMENTAL RESULTS

The proposed scheme was evaluated using the MORPH II [26] and CACD dataset [27], as these large scale datasets provide the subjects’ identities. This allows us to apply the Subject-Exclusive (SE) protocol. The previously used Random Selection (RS) evaluation protocol allows images of the same subject to be in both train and test datasets. This results in train-test leakage, effectively turning the task into a face-matching problem [22]. The MORPH II [26] is one of the most extensive longitudinal face databases available, containing 55,134 facial images with known identities showing 13,617 subjects between 16 and 77 old. Each subject is shown in multiple mugshots captured under controlled conditions. The dataset includes individuals of both genders and diverse ethnicities, primarily White and Black, with demographic and gender distributions detailed in Table I. The Cross-Age Celebrity Dataset (CACD) dataset contains 163,446 images of 2,000 celebrities aged 14 to 62, retrieved from the Internet, with identities provided for each image. The age was determined by subtracting the celebrity’s birth year from the year the photo was taken.

Gender	Black	White	Asian	Hispanic	Other
Male	36,832	7,961	141	1,667	44
Female	5,757	2,598	13	102	19
Total	42,589	10,559	154	1,769	63

TABLE I: Demographic breakdown of the MORPH II [26] dataset.

We evaluated age estimation accuracy using Mean Absolute Error (MAE), consistent with prior studies [22].

$$MAE = \frac{1}{N} \sum_{i=1}^N |\hat{a}_q^i - a_q^i|, \quad (7)$$

where \hat{a}_q^i and a_q^i are the predicted and ground truth age, respectively.

To allow a fair comparison with previous works [22], the VGG-16 backbone [45] was used. Our approach was trained in three phases. The first, was to fine-tune the backbone (initialized with pre-trained ImageNet weights) to face recognition using the corresponding training set (either Morph II [26] or CACD [27]) and the ArcFace loss [47]. In the second, we compute the image embeddings of the VGG-16 backbone. Last, the third phase uses the initial BAR result to train the proposed DAR approach introduced in Section III.

We used the same training and test sets to train the BAR and DAR models. The training set is divided into two subject-exclusive parts, as in Section III-A: a distribution estimation set (2% of the training set) and the model training dataset, used for both the BAR and the DAR scheme. The input face images are resized to 224×224 , intensity normalized to $[0, 255]$, and augmented by randomly applying each with a 0.5 probability: horizontal flipping, color jittering, random affine transformation, and random small-part erasure. We used $R = 10$ references randomly selected from the nearest neighbor pool of size $P = 30$. We used the Ranger optimizer [48] and learning rate scheduling using Cosine Annealing. The experiments were conducted on dual NVIDIA Tesla V100 GPUs, with the code implemented using the PyTorch framework. The iterative improvement framework was applied using two iterations of the training process.

A. Results

We compared our approach with SOTA methods that are detailed in Tables II and III. We report their published results, ensuring adherence to the SE protocol, consistent with our methodology. We use the same 80% training and 20% testing split and SE protocol as in prior works [22], where our training set was split to 78% training and 2% of the data for estimating the BAR error distribution D_ϵ as in Section III-A. Table II presents the MORPH II dataset results, demonstrating that our approach outperforms previous methods under the SE protocol, achieving a new state-of-the-art MAE of 2.47. The method also achieves superior performance on the CACD dataset, with an MAE of 5.27. Figures 6 and 7 illustrate the error distribution of our proposed age estimation scheme, which closely approximates a Gaussian distribution.

Method	Backbone	MAE	Protocol
Coral[35]	RESNET34	3.27	SE
Mean-Variance[31]	VGG16	2.79	SE
soft-ranking[20]	RESNET34	2.83	SE
soft-ranking[20]	VGG16	2.71	SE
DCDL[36]	VGG-16-BN	2.62	SE
Hierarchical-Attention[22]	VGG16	2.53	SE
Ours	VGG16	2.47	SE

TABLE II: Age estimation results evaluated using the MORPH II [26] dataset, encompassing our results compared with previous SOTA approaches using the SE protocol.

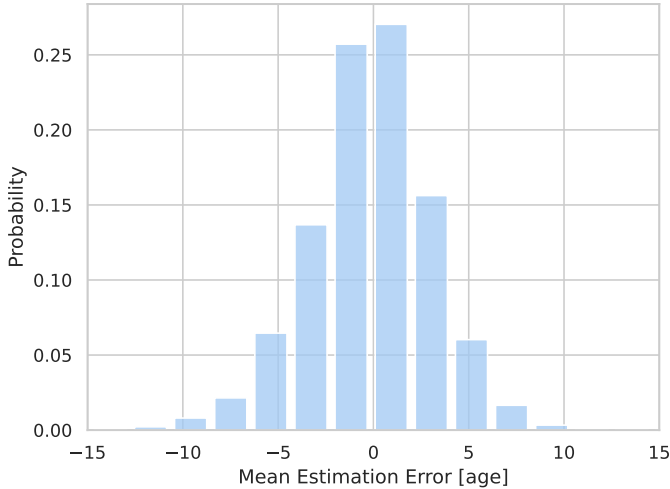


Fig. 6: Distribution of mean error for the proposed method, over the Morph II dataset.

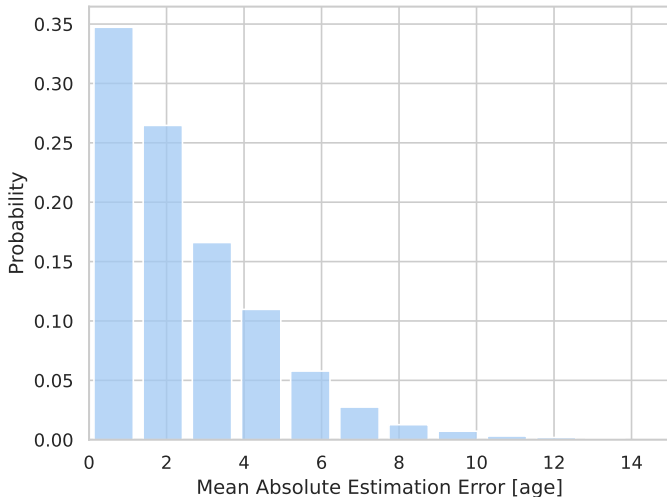


Fig. 7: Distribution of mean absolute error for the proposed method, over the Morph II dataset.

B. Ablation Study

We conducted an ablation study to evaluate the contributions of key components in our approach. In each experiment, a specific algorithmic property or hyperparameter was systematically varied across a predefined range, followed by training and evaluation using the MORPH II dataset and the established protocol. First, we examined the impact of the number of

Method	Backbone	MAE	Protocol
Hierarchical-Attention(CNN)[22]	VGG16	5.80	SE
Hierarchical-Attention[22]	VGG16	5.35	SE
Ours	VGG16	5.27	SE

TABLE III: Age estimation results evaluated using the CACD [27] dataset, encompassing our results compared with previous SOTA approaches using the SE protocol.

retrieved references R from the nearest-neighbor pool (size $P = 30$), as summarized in Table IV. While the number of selected references influences performance, no clear trend emerges. Interestingly, increasing the number of references ($R > 1$) does not consistently improve estimation accuracy.

#Refs	MAE
1	2.5
2	2.47
5	2.51
10	2.47

TABLE IV: Ablation study of the number of references used by the retrieval.

We further analyzed the reference retrieval strategy. After determining the target reference age, we compared two selection methods: random sampling and nearest-neighbor-based retrieval. In the random-based method, references are uniformly selected out of the entire collection of face images of the selected reference age. In contrast, in the nearest-neighbor-based selection the references are selected using the L_2 norm embedding distance (see Section III-A). To ensure query-reference dataset diversity and reduce overfitting, the nearest-neighbor selection first selects a pool of P references, from which a subset is then randomly and uniformly selected. The results, summarized in Table V, indicate that the nearest-neighbor retrieval method consistently enhances MAE accuracy.

Retrieval Method	#Refs	MAE
Random	10	2.5
Nearest Neighbor	10	2.47

TABLE V: Ablation study of the reference set retrieval approach.

We studied the contribution of the error distribution estimate used to sample reference training samples in Section III-A. For that, we compared two methods. The first is a baseline approach where the references were sampled from a $U(-3,3)$ discrete uniform distribution. The second method uses the proposed KDE-based. The results are summarized in Table VI showing that the KDE approach is superior. We also found that the uniform distribution-based method converged notably slower (300 epochs) compared to the KDE-based method (150 epochs).

Error Distribution	#Refs	MAE
$U(-3,3)$	2	2.51
KDE	2	2.47

TABLE VI: Ablation study of the distribution estimate used to sample the age differences.

The Differential Age Regression (DAR) network in Section III-B uses a set of regression heads $\{R_c\}_{-C}^C$ that estimate the

second-order differences and are probabilistically weighted. In this ablation, we compare this approach to a simple difference classifier. We show the results of using a single and two iterations, as in Section III-D. It follows that the use of the regression cascade provides a slight, but consistent improvement.

ADR Method	Iteration	
	#1	#2
Classifier	2.49	2.48
Regressors + Classifier	2.50	2.47

TABLE VII: Ablation study of the Differential Age Regression (DAR) network (Section III-B). We compare our scheme to using an age-differential classifier, without the additional set of regressors.

Finally, we evaluated the iterative improvement proposed in Section III-D. We present the results of an iterative improvement using two training refinement steps: training, saving the results over the distribution set, and retraining based on these results to refine the first phase. We used KDE and $R = 10$ references, as this configuration achieved SOTA results. The results are summarized in Table VIII, and it is worth noting that we also experimented with multiple learning rates in the second iteration.

Error Distribution	#Refs	Iteration	Learning Rate	MAE
KDE	10	1	0.0003	2.5
KDE	10	2	0.0003	2.47

TABLE VIII: Ablation study of the iterative refinement using single and two iterations.

V. BIAS ANALYSIS

We conducted a statistical bias analysis of our proposed scheme using the MORPH II dataset, whose gender and ethnicity distributions are detailed in Table I. Our methodology follows the approach outlined by Hiba and Keller [22]. As the MORPH II dataset exhibits imbalances in age, gender, and ethnicity, and our approach relies on random sampling, the resulting training and test sets inherit these biases. We analyze the bias introduced by our scheme, despite achieving SOTA accuracy under the SE protocol, to better understand its implications.

Age bias. Table IX reports the error distribution for different age ranges. We report the number of training samples per age range, as the error relates to the number of training samples. The lowest error is observed for the 15-24 age range. As the number of training samples in these bins (15-19 and 20-24) is comparable to some older age ranges that exhibit higher estimation errors, this suggests that lower errors are primarily due to appearance variations rather than sample size alone. However, the number of samples also contributes to the predictive power. Age estimation error remains relatively stable for midlife ages (30-50) but increases significantly for

Age	#Samples	MAE	STD
15-19	5961	1.62	1.88
20-24	7320	2.01	2.59
25-29	5619	2.49	3.15
30-34	5630	2.73	3.45
35-39	6905	2.59	3.34
40-44	5772	2.64	3.29
45-49	3879	3.02	3.49
50-54	2182	3.25	3.47
55-59	753	4.58	3.43
60-64	192	5.67	3.09
65-69	56	9.56	1.45

TABLE IX: **Age bias.** Each row presents a separate age range bin, its amount of training samples, and the resulting test MAE and standard deviation of the age estimation error.

older age groups (55+), where the availability of training samples is substantially lower.

Gender and ethnicity bias. Gender and ethnicity are the most common sources of estimation bias in biometrics use cases [49]. Figures 8 and 9 examine the ethnicity bias. We present the mean error and MAE histogram across all ethnicities. The MORPH II database is heavily skewed towards Black men, who make up 67% of the dataset. In Figures 10 and 11, we present the gender bias analysis. The MAE for men is about 24% lower than that of women, resulting from the larger number of male training samples.

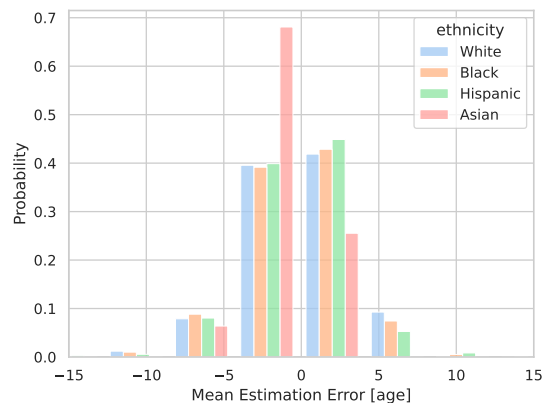


Fig. 8: **Ethnicity bias (error histogram).** Distribution of mean error for our proposed method, over the Morph II dataset, across the different ethnicities in the dataset.

Figures 12 and 13 present the estimation bias across both gender and ethnicity, indicating the error and MAE per each ethnicity class and gender. The MAE for female subjects is greater across all ethnicities, except for the Asian ethnicity. The MAE across the various ethnicity classes is much more uniform, with noticeably smaller variability for men, compared to women.

VI. CONCLUSIONS

We propose a novel framework for age estimation from facial images. First, we introduce a differential age estimation approach that trains an age difference estimator, using a query

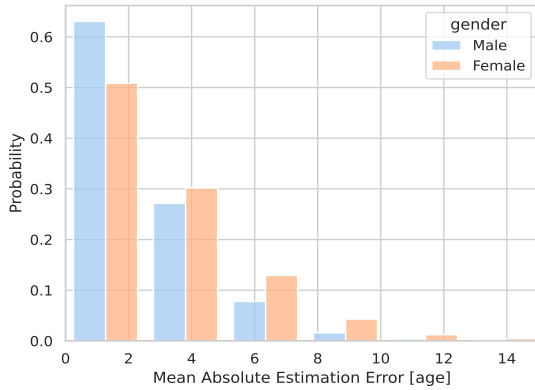


Fig. 11: **Gender bias (MAE histogram)**. A gender-wise distribution of MAE for our proposed method, over the Morph II dataset.

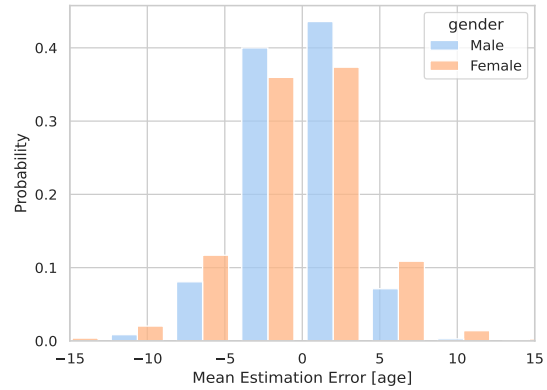


Fig. 10: **Gender bias (error histogram)**. A gender-wise distribution of mean error for our proposed method, using the Morph II dataset.

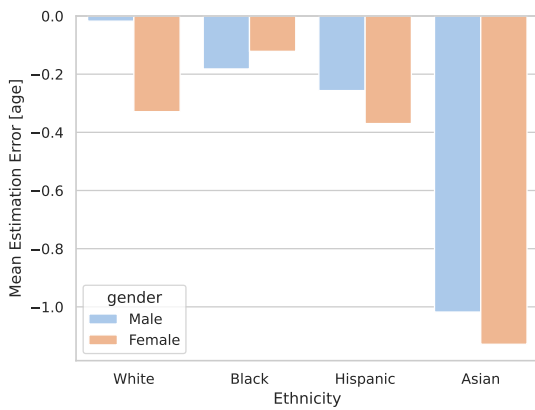


Fig. 12: **Gender and ethnicity bias**. A per-ethnicity and gender breakdown of the mean error for our proposed method, using the Morph II dataset.

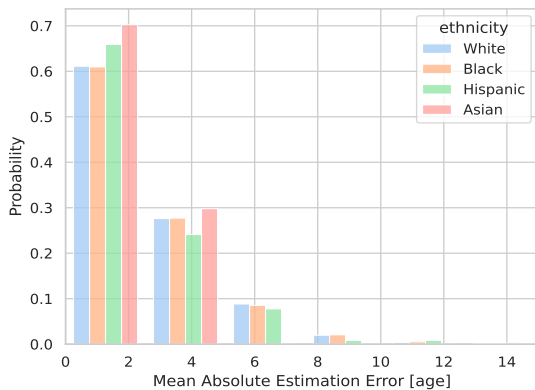


Fig. 9: **Ethnicity bias (MAE histogram)**. Distribution of the MAE of our proposed method, using the Morph II dataset, across the different ethnicities in the dataset.

image and a set of reference images retrieved by a baseline age estimator. Second, we enhance the baseline age estimator by Kernel Density Estimation (KDE) to effectively sample reference images, improving the diversity and relevance of the reference set. The individual age estimations for each reference image are aggregated using learned probabilistic weights to produce the final age estimate. To our knowledge, ours is the first work to present a differential age estimation scheme. We also propose an iterative refinement of the BAR error estimate, which further enhances the accuracy of the age predictions. Experimental results demonstrate that our approach outperforms existing SOTA methods.

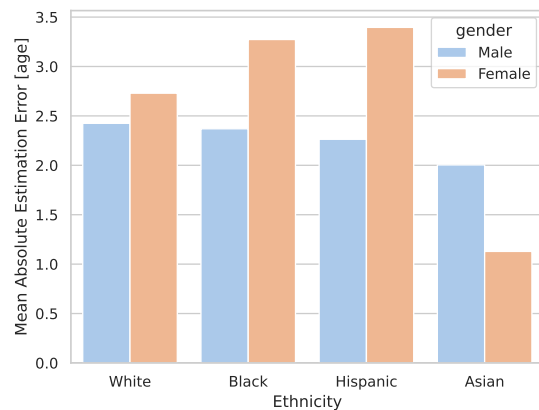


Fig. 13: **Gender bias (MAE histogram)**. A per-ethnicity and gender breakdown of MAE for our proposed method, using the Morph II dataset.

REFERENCES

- [1] A. Hakeem, H. Gupta, A. Kanaujia, T. E. Choe, K. Gunda, A. W. Scanlon, L. Yu, Z. Zhang, P. L. Venetianer, Z. Rasheed, and N. Haering, "Video analytics for business intelligence," in *Video Analytics for Business Intelligence*, 2012.
- [2] A. Lanitis, C. Draganova, and C. Christodoulou, "Comparing different classifiers for automatic age estimation," *IEEE Transactions on Systems, Man, and Cybernetics, Part B (Cybernetics)*, vol. 34, pp. 621–628, 2004.
- [3] V. Lambros, "Facial aging: A 54-year, three-dimensional population study," *Plastic and reconstructive surgery*, vol. 145, pp. 921–928, 04 2020.
- [4] E. Eidinger, R. Enbar, and T. Hassner, "Age and gender estimation of unfiltered faces," *IEEE Transactions on Information Forensics and Security*, vol. 9, no. 12, pp. 2170–2179, 2014.
- [5] G. Guo and G. Mu, "Simultaneous dimensionality reduction and human age estimation via kernel partial least squares regression," in *Proceedings of the IEEE/CVF Conference on Computer Vision and Pattern Recognition (CVPR)*, June 2011, pp. 657–664.
- [6] K.-Y. Chang, C.-S. Chen, and Y.-P. Hung, "Ordinal hyperplanes ranker with cost sensitivities for age estimation," in *Proceedings of the IEEE/CVF Conference on Computer Vision and Pattern Recognition (CVPR)*, June 2011, pp. 585–592.
- [7] D. Cao, Z. Lei, Z. Zhang, J. Feng, and S. Z. Li, "Human age estimation using ranking svm," in *Biometric Recognition*, W.-S. Zheng, Z. Sun, Y. Wang, X. Chen, P. C. Yuen, and J. Lai, Eds. Berlin, Heidelberg: Springer Berlin Heidelberg, 2012, pp. 324–331.
- [8] E. Ramón-Balmaseda, J. Lorenzo-Navarro, and M. Castrillón-Santana, "Gender classification in large databases," in *Progress in Pattern Recognition, Image Analysis, Computer Vision, and Applications*. Springer, 2012, pp. 74–81.
- [9] G. Guo and G. Mu, "Human age estimation: What is the influence across race and gender?" in *IEEE Conference on Computer Vision and Pattern Recognition Workshops (CVPRW)*, June 2010, pp. 71–78.
- [10] X. Wang and C. Kamhamettu, "Age estimation via unsupervised neural networks," in *International Conference on Automatic Face and Gesture Recognition (FGR)*, vol. 1, May 2015, pp. 1–6.
- [11] K. Chen, S. Gong, T. Xiang, and C. Loy, "Cumulative attribute space for age and crowd density estimation," in *Proceedings of the IEEE/CVF Conference on Computer Vision and Pattern Recognition (CVPR)*, June 2013, pp. 2467–2474.
- [12] G. Levi and T. Hassner, "Age and gender classification using convolutional neural networks," in *IEEE Conference on Computer Vision and Pattern Recognition Workshops (CVPRW)*, June 2015, pp. 34–42.
- [13] H. Liu, J. Lu, J. Feng, and J. Zhou, "Label-sensitive deep metric learning for facial age estimation," *IEEE Transactions on Information Forensics and Security*, vol. 13, no. 2, pp. 292–305, 2018.
- [14] O. Sendik and Y. Keller, "Deepage: Deep learning of face-based age estimation," *Signal Processing: Image Communication*, vol. 78, 08 2019.
- [15] R. Hadsell, S. Chopra, and Y. LeCun, "Dimensionality reduction by learning an invariant mapping," in *Proceedings of the IEEE/CVF Conference on Computer Vision and Pattern Recognition (CVPR)*, vol. 2, 2006, pp. 1735–1742.
- [16] K. Li, J. Xing, C. Su, W. Hu, Y. Zhang, and S. Maybank, "Deep cost-sensitive and order-preserving feature learning for cross-population age estimation," in *Proceedings of the IEEE/CVF Conference on Computer Vision and Pattern Recognition (CVPR)*, 2018, pp. 399–408.
- [17] Q. Tian, M. Cao, S. Chen, and H. Yin, "Relationships self-learning based gender-aware age estimation," *Neural Processing Letters*, vol. 50, no. 3, pp. 2141–2160, 2019.
- [18] S. Chen, C. Zhang, M. Dong, J. Le, and M. Rao, "Using ranking-cnn for age estimation," in *Proceedings of the IEEE/CVF Conference on Computer Vision and Pattern Recognition (CVPR)*, 2017, pp. 742–751.
- [19] Z. Niu, M. Zhou, L. Wang, X. Gao, and G. Hua, "Ordinal regression with multiple output cnn for age estimation," in *Proceedings of the IEEE/CVF Conference on Computer Vision and Pattern Recognition (CVPR)*, 2016, pp. 4920–4928.
- [20] X. Zeng, J. Huang, and C. Ding, "Soft-ranking label encoding for robust facial age estimation," *IEEE Access*, vol. 8, pp. 134 209–134 218, 2020.
- [21] Q. Zhao, J. Dong, H. Yu, and S. Chen, "Distilling ordinal relation and dark knowledge for facial age estimation," *IEEE Transactions on Neural Networks and Learning Systems*, vol. PP, 07 2020.
- [22] S. Hiba and Y. Keller, "Hierarchical Attention-Based Age Estimation and Bias Analysis," *IEEE Transactions on Pattern Analysis and Machine Intelligence*, vol. 45, no. 12, pp. 14 682–14 692, Dec. 2023.
- [23] H. Wang, V. Sánchez, and C.-T. Li, "Improving face-based age estimation with attention-based dynamic patch fusion," *IEEE Trans. Image Process.*, vol. 31, pp. 1084–1096, 2022.
- [24] Y. Lin, J. Shen, Y. Wang, and M. Pantic, "Fp-age: Leveraging face parsing attention for facial age estimation in the wild," 2021.
- [25] A. Ali, A. Marisetty, and F. Brémond, "P-age: Pexels dataset for robust spatio-temporal apparent age classification," in *IEEE Workshop on Applications of Computer Vision*, January 2024, pp. 8606–8615.
- [26] K. Ricanek and T. Tesafaye, "Morph: a longitudinal image database of normal adult age-progression," in *International Conference on Automatic Face and Gesture Recognition (FGR)*, 2006, pp. 341–345.
- [27] B.-C. Chen, C.-S. Chen, and W. H. Hsu, "Cross-age reference coding for age-invariant face recognition and retrieval," in *Proceedings of the European Conference on Computer Vision (ECCV)*, D. Fleet, T. Pajdla, B. Schiele, and T. Tuytelaars, Eds. Cham: Springer International Publishing, 2014, pp. 768–783.
- [28] H. Han, C. Otto, and A. Jain, "Age estimation from face images: Human vs. machine performance," in *International Conference on Biometrics*, June 2013, pp. 1–8.
- [29] J. Buolamwini and T. Gebru, "Gender shades: Intersectional accuracy disparities in commercial gender classification," in *Proceedings of the 1st Conference on Fairness, Accountability and Transparency*, S. A. Friedler and C. Wilson, Eds., vol. 81, 2018, pp. 77–91.
- [30] R. Rothe, R. Timofte, and L. Van Gool, "Dex: Deep expectation of apparent age from a single image," in *Proceedings of the IEEE International Conference on Computer Vision Workshops (ICCVW)*, 2015, pp. 252–257.
- [31] H. Pan, H. Han, S. Shan, and X. Chen, "Mean-variance loss for deep age estimation from a face," in *Proceedings of the IEEE/CVF Conference on Computer Vision and Pattern Recognition (CVPR)*. IEEE Computer Society, 2018, pp. 5285–5294.
- [32] X. Yang, B. Gao, C. Xing, Z. Huo, X. Wei, Y. Zhou, J. Wu, and X. Geng, "Deep label distribution learning for apparent age estimation," in *Proceedings of the IEEE International Conference on Computer Vision Workshops (ICCVW)*, 2015, pp. 344–350.
- [33] W. Shen, Y. Guo, Y. Wang, K. Zhao, B. Wang, and A. Yuille, "Deep regression forests for age estimation," in *Proceedings of the IEEE/CVF Conference on Computer Vision and Pattern Recognition (CVPR)*, 2018, pp. 2304–2313.
- [34] W. Li, J. Lu, J. Feng, C. Xu, J. Zhou, and Q. Tian, "Bridgenet: A continuity-aware probabilistic network for age estimation," in *Proceedings of the IEEE/CVF Conference on Computer Vision and Pattern Recognition (CVPR)*, 2019, pp. 1145–1154.
- [35] W. Cao, V. Mirjalili, and S. Raschka, "Rank consistent ordinal regression for neural networks with application to age estimation," *Pattern Recognition Letters*, vol. 140, pp. 325–331, 2020.
- [36] H. Sun, H. Pan, H. Han, and S. Shan, "Deep conditional distribution learning for age estimation," *IEEE Transactions on Information Forensics and Security*, vol. 16, pp. 4679–4690, 2021.
- [37] Z. Bao, Z. Tan, J. Li, J. Wan, X. Ma, and Z. Lei, "General vs. long-tailed age estimation: An approach to kill two birds with one stone," *IEEE Trans. Image Process.*, vol. 32, p. 6155–6167, Jan. 2023.
- [38] H. Liu, M. Ma, Z. Gao, Z. Deng, F. Li, and Z. Li, "Siamese graph learning for semi-supervised age estimation," *IEEE Trans. Multimedia*, vol. 25, pp. 9586–9596, 2023.
- [39] P. Chen, X. Zhang, Y. Li, J. Tao, B. Xiao, B. Wang, and Z. Jiang, "Daa: A delta age adain operation for age estimation via binary code transformer," in *Proceedings of the IEEE/CVF Conference on Computer Vision and Pattern Recognition (CVPR)*, 2023.
- [40] P. Phillips, H. Wechsler, J. Huang, and P. J. Rauss, "The FERET database and evaluation procedure for face-recognition algorithms," *Image and Vision Computing*, vol. 16, no. 5, pp. 295–306, 1998.
- [41] T. Cootes and A. Lanitis, "The fg-net aging database," 2002, available online at <http://www-prima.inrialpes.fr/FGnet/>.
- [42] E. Agustsson, R. Timofte, S. Escalera, X. Baro, I. Guyon, and R. Rothe, "Apparent and real age estimation in still images with deep residual regressors on appa-real database," in *International Conference on Automatic Face and Gesture Recognition (FGR)*. IEEE, 2017.
- [43] Zhang, Zhifei, Song, Yang, Qi, and Hairong, "Age progression/regression by conditional adversarial autoencoder," in *Proceedings of the IEEE/CVF Conference on Computer Vision and Pattern Recognition (CVPR)*. IEEE, 2017, pp. 4352–4360.
- [44] K. Ricanek and T. Tesafaye, "Morph: a longitudinal image database of normal adult age-progression," in *International Conference on Automatic Face and Gesture Recognition (FGR)*, April 2006, pp. 341–345.
- [45] K. Simonyan and A. Zisserman, "Very deep convolutional networks for large-scale image recognition," in *Proceedings of the International Conference on Learning Representations (ICLR)*, Y. Bengio and Y. LeCun, Eds., 2015.

- [46] B. W. Silverman, *Density Estimation for Statistics and Data Analysis*, ser. Monographs on Statistics and Applied Probability. London: Chapman and Hall, 1986.
- [47] J. Deng, J. Guo, J. Yang, N. Xue, I. Kotsia, and S. Zafeiriou, "Arcface: Additive angular margin loss for deep face recognition," *IEEE Transactions on Pattern Analysis and Machine Intelligence*, vol. 44, no. 10, p. 5962–5979, Oct. 2022.
- [48] L. Wright and N. Demeure, "Ranger21: a synergistic deep learning optimizer," *CoRR*, vol. abs/2106.13731, 2021. [Online]. Available: <https://arxiv.org/abs/2106.13731>
- [49] J. P. Robinson, G. Livitz, Y. Henon, C. Qin, Y. Fu, and S. Timoner, "Face recognition: too bias, or not too bias?" in *IEEE Conference on Computer Vision and Pattern Recognition Workshops (CVPRW)*, 2020, pp. 0–10.